FINAL TECHNICAL REPORT:
SCEC Award Number 17136
Crack models to constrain time-dependent interseismic slip-rate distributions from geodetic data

Paul Segall
Geophysics Department, Stanford University
Email: segall@stanford.edu

Lucile Bruhat
Geophysics Department, Stanford University
Email: lbruhat@stanford.edu

Proposal year: 2017

August 20, 2019

Abstract

Most inversions consider the depth distribution of interseismic fault slip-rate to be time invariant. However, some numerical simulations show penetration of dynamic rupture into regions with velocity-strengthening friction, with subsequent interseismic up-dip propagation of the locked-to-creeping transition. We explored this hypothesis by developing and testing crack models to describe creep penetration upward into the locked region. Previous work from *Bruhat and Segall* (2017) developed a new method to characterize interseismic slip rates, that does not assume that the spatial distribution of interseismic slip is stationary. This simple model considers deep interseismic slip as a crack loaded at specified slip rate at the down-dip end. It provides analytical expressions for stress drop within the crack, slip, and slip rate along the fault.

This work extended this new class of solution to strike-slip fault environment. Unlike *Bruhat and Segall* (2017) which considered creep propagation in a fully elastic medium, we included here the long-term deformation due to viscoelastic flow in the lower crust and upper mantle. We improved the model presented in *Bruhat and Segall* (2017) to account for the coupling between creep and viscoelastic flow, and derived expression for viscoelastic response due to time-dependent creep. Finally, we employed this model to investigate the long-term rates along the Carrizo Plain section of the San Andreas fault. A paper describing this work is now in review.

1 Report

The earliest models for interseismic deformation described a fault as a single screw dislocation in an elastic half-space, locked to some depth, but slipping at a constant rate below. Using this

model, kinematic inversions of geodetic surface rates have, for decades, been used to estimate the locking depth, presumed to delimit the deep extent of the seismogenic region.

Bruhat and Segall (2017) recently developed a new method to characterize interseismic slip rates, that allows slip to penetrate up dip into the locked region. This simple model considered deep interseismic slip as a crack loaded at constant slip rate at the down-dip end. We provided analytical expressions for stress drop within the crack, slip, and slip rate along the fault, and enabled inversions for physical characteristics of the fault interface, bridging purely kinematic inversions to physics-based numerical simulations of earthquake cycles.

In this study, we apply this model of propagating deep interseismic creep to strike-slip earthquake cycle models. Unlike *Bruhat and Segall* (2017) which considered creep propagation in a fully elastic medium, we include here the long-term deformation due to cyclic earthquake ruptures on a fault in an elastic crust, overlying a viscoelastic medium.

Propagating crack models for viscoelastic strike-slip earthquake cycle models

Consider a strike-slip fault embedded in an elastic layer of thickness H, overlying a Maxwell viscoelastic half-space (Figure 1). The fault is partially locked during the interseismic period, but slips below. Every T years, an earthquake partly ruptures the fault section. The sum of seismic and aseismic slip must keep pace with the far-field motion. Thus, the maximum coseismic displacement is $\Delta u = Tv^{\infty}$.

Surface rates $\mathbf{v_{horz}}$ result from 1) cumulative effects of the viscoelastic earthquake cycle $\mathbf{v_{EQcycle}}$, and 2) the elastic and viscoelastic responses due to interseismic creep, respectively $\mathbf{v_{elcreep}}$ and $\mathbf{v_{vecreep}}$:

$$\mathbf{v_{horz}} = \mathbf{v_{EQcycle}} + \mathbf{v_{elcreep}} + \mathbf{v_{vecreep}}.$$

While expression for $\mathbf{v_{EQcycle}}$ can be found in *Savage and Prescott* (1978) and *Segall* (2010, Sections 6.3 and 12.4.1), we derive expressions for the elastic and viscoelastic responses due to interseismic creep.

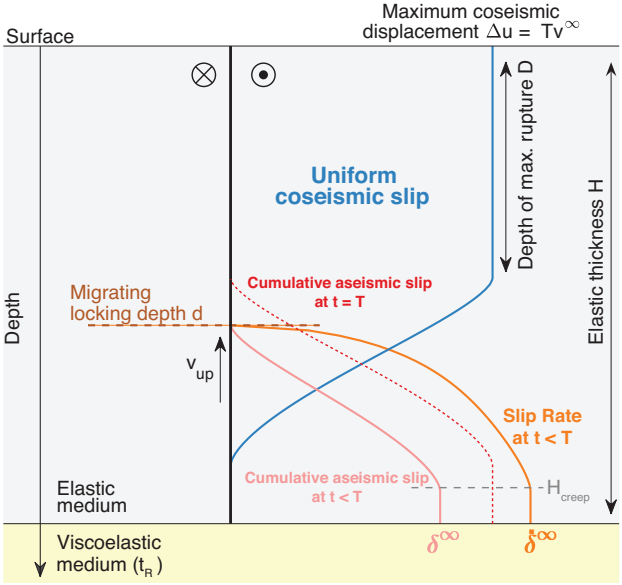

Figure 1: Model set-up for this study. The fault accommodates long-term plate rate v^{∞}. Every T years, an earthquake ruptures the upper part of the elastic crust. Maximum coseismic slip is given by Tv^{∞}. During the interseismic period, the deeper part of the fault creeps, pushing the locking depth up.

Crack models for interseismic creep

Consider a 1D crack of length a, extending vertically in the elastic layer and loaded by displacement $\delta^{\infty}(t)$ at the top of the viscoelastic medium (see Figure 1). We follow the same approach developed in *Bruhat and Segall* (2017) who expanded the stress drop within the crack in Chebyshev polynomials of the first kind T_i:

$$\Delta\tau(\xi,t) = \mu\sum_{i=0}^{\infty} c_i T_i(\xi), \tag{1}$$

where c_i are the coefficients of the Chebyshev polynomials, and ξ is a normalized spatial variable such that $\xi \in [-1,1]$. For a non-singular crack driven at steady displacement, *Bruhat and Segall*

(2017) derived values of the coefficients c_i for $i = 0, 1$. This methodology provides expressions for slip, slip rate, stress and stress rate within the crack. Since the bottom end of the crack is anchored to the upper limit of the viscoelastic medium, the displacement and velocity boundary conditions must reflect the viscoelastic response of the mantle. We approximate the displacement and velocity boundary conditions as δ^∞ and $\dot{\delta}^\infty$, assuming a first-order expansion of the series in *Segall* (2010, Section 12.4.1):

$$\delta^\infty = = v^\infty T\Big(\frac{e^{-T/t_R}}{e^{-T/t_R}-1}\Big)(1-e^{-t/t_R}), \tag{2a}$$

$$\dot{\delta}^\infty = \frac{v^\infty T}{t_R}\Big(\frac{e^{-T/t_R}}{e^{-T/t_R}-1}\Big)e^{-t/t_R}. \tag{2b}$$

where t_R is the Maxwell relaxation time.

Viscoelastic response from time-varying interseismic creep

We then develop a method to compute the viscoelastic response due to time-varying slip rates below the locked region. Consider $\dot{s}(t)$ the slip rate distribution along the fault within the region defined between the deep extent of earthquake rupture D and the top of the viscoelastic layer H. Following *Savage and Prescott* (1978) and *Segall* (2010, Section 12.4.1), the viscoelastic response associated with slip-rate $\dot{s}_i(t)$ at depth z_i, due to successive earthquakes at times t' extending from $-\infty$ to current time t is:

$$\hat{v}_i(x,t) = \frac{1}{\pi}\sum_{n=1}^{\infty}\frac{G_n(x,z_i,H)}{(n-1)!}\int_{-\infty}^{t}\dot{s}_i(t')e^{-(t-t')/tR}\Big(\frac{t-t'}{t_R}\Big)^{n-1}dt', \tag{3}$$

where G_n is the spatial operator defined by:

$$G_n(x,z_i,H) = F_n(x,z_{i+1},H) - F_n(x,z_i,H), \tag{4a}$$

$$\text{and} \quad F_n(x,z_i,H) = \tan^{-1}\left(\frac{2nH-z_i}{x}\right) - \tan^{-1}\left(\frac{2nH+z_i}{x}\right). \tag{4b}$$

We assume that the slip rate distribution $\dot{s}(t)$ can be expressed as the sum of the long-term plate motion rate and a time-dependent term:

$$\dot{s}(t) = \begin{cases} v^\infty + \Delta\dot{s}(t) & \text{when } t \geq 0 \\ v^\infty & \text{when } t < 0 \end{cases} \tag{5}$$

The steady part v^∞ applies to all past earthquake cycles, whereas the time-dependent term corresponds to the present cycle. Substituting this expression into equation (3) leads to:

$$\hat{v}_i(x,t) = \frac{1}{\pi}\sum_{n=1}^{\infty}G_n(x,z_i,H)\Big(v^\infty + \frac{1}{(n-1)!}\int_0^t\Delta\dot{s}_i(t')e^{-(t-t')/tR}\Big(\frac{t-t'}{t_R}\Big)^{n-1}dt'\Big). \tag{6}$$

Equation (6) gives the expression of the cumulative effect of viscoelastic flow due to time-dependent creep. This approximation is compared to results from *Johnson and Segall* (2004) who computed slip and slip rate within the creeping region through a boundary element approach for a fault subject to constant shear stress.

Figure 2 displays slip rate profiles along depth and surface displacement rate profiles as a function of distance perpendicular to the fault due to elastic and viscoelastic response. These profiles are computed at five times during the interseismic period, and for two relaxation times t_R. Here the creeping region is described following the crack model described above, by a crack lying initially between 18 and 25 km, migrating vertically at 10 m/year. At $t = 0$ the viscoelastic response is the same as the solution for a region creeping at constant rate v^∞. Depending on the relaxation time, the behavior early in the interseismic period varies. Later in the cycle, the amplitude of the viscoelastic response decreases with time and distance.

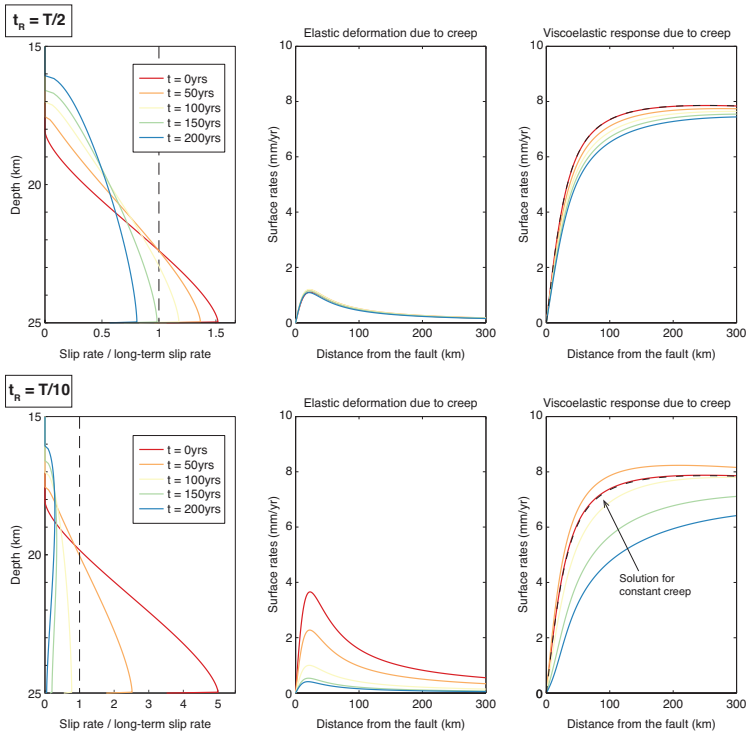

Figure 2: Elastic and viscoelastic deformation induced by time-varying creep when $t_R = T/2$ and $t_R = T/10$. The creeping region is described by a crack lying initially between 18 and 25 km, migrating vertically at 10 m/year. Left panels show the slip rate profiles as a function of depth. Middle panels show the elastic surface velocity due to interseismic creep. Right panels give the viscoelastic surface velocity using equation (6). Dashed back line is the solution for creep at constant rate v^∞.

Application to the Carrizo Plain segment of the San Andreas fault

We apply this model to horizontal long-term rates in Central California provided by the SCEC Crustal Motion Model Map 4.0 published in *Shen et al.* (2011). Stations perpendicular to the Carrizo Plain section of the San Andreas fault are then selected (Figure 3).

This study developed inverse methods to test different models of interseismic deformation, in some cases accounting for propagating deep slip. We first found best fitting solutions for classical models that consider the fault to be either a single dislocation in a fully elastic medium, or models that include a region of steady creep above a viscoelastic region. We also consider solutions based on the boundary element method developed by *Johnson and Segall* (2004). We finally apply the method developed here including propagating deep interseismic creep. Inversions solve for the elastic thickness H, the depth of uniform rupture D, the locking depth, defined by the top of the creeping region d, the long-term plate motion rate v^∞, the viscoelastic relaxation time t_R, and the maximum coseismic displacement Δu, related to the earthquake recurrence time T (see Figure 1). The migration speed v_{up} is defined such that the creeping region reaches the down dip limit of maximum coseismic slip at the end of the earthquake cycle.

To ensure that at the end of the cycle, slip along the entire fault is equal to the imposed far-field displacement, the coseismic slip distribution is defined as the complement of the aseismic slip distribution at the end of the cycle. Finally, in order to be consistent with the depth distribution of microseismicity, we consider solutions whose peak in stress rate lies in the same region as the

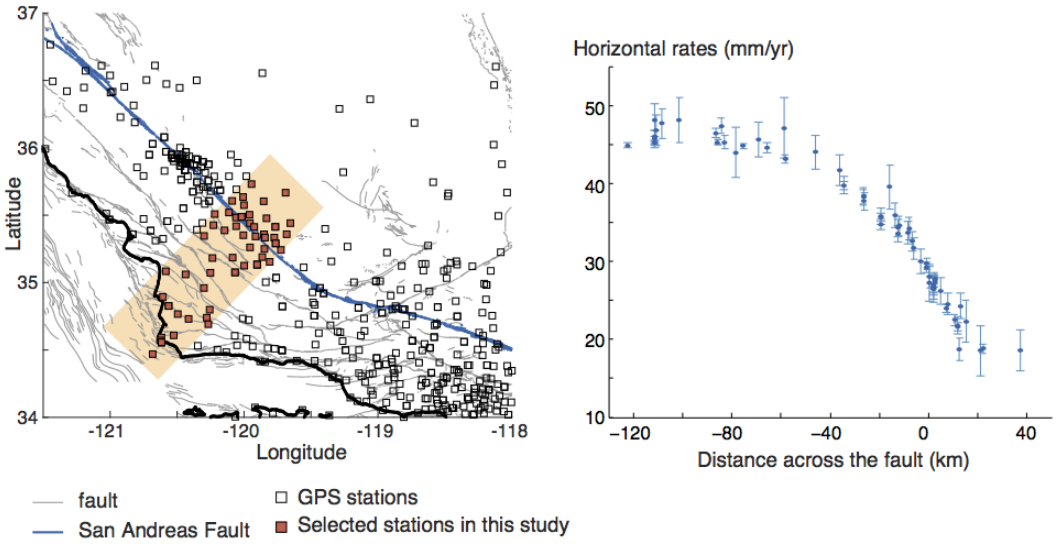

Figure 3: Data set used in this study. Left: Map of central and southern California fault system with selected stations. The San Andreas fault is denoted in blue. Right: Fault parallel component of interseismic velocities relative to the North American plate for the selected stations.

current seismicity (between 8–13 km). This is an important point in our inversion. Our updated model allow us to derive the distribution of shear stress rate within the creeping region. While our inversion is directed by horizontal geodetic velocities, we assume that the location of maximum shear stressing rate should coincide with the region of largest moment release from the microseismicity. We employ Markov Chain Monte Carlo (MCMC) methods for the inversions. MCMC algorithms efficiently estimate the maximum-likelihood solution and enable the construction of posterior distributions.

Best fitting models are displayed in Figures 4 and 5. Our best fitting solutions suggest uniform coseismic slip to a depth of 10 km, then slowly tapering to zero at 15-20 km (Figure 5). Interseismic creep is restricted to between ≈10 km and the top of the viscoelastic layer and can potentially migrate vertically at speeds up to 10 m/year. Estimates of elastic thickness vary from 18 to 23 km. This model exhibits positive stress rate within the same region than the current microseismicity.

Figure 4 shows that the differences in fit are limited. Our improved model shows, however, a better range for the likelihood, compared to all other inversions. We also compute the deviance information criterion (DIC) (*Spiegelhalter et al.*, 2002) to compare the fits. The DIC is a way of measuring model fit, similar to Akaike information criterion (AIC), but for MCMC solutions. Models with lower DIC give the best estimated solutions. In this study, although we increased the number of parameters, our improved model has a DIC lower than all the other inversions.

Compared to the model with constant creep from *Savage and Prescott* (1978) and the boundary element model developed by *Johnson and Segall* (2004), we present a kinematic model that allows the spatial migration of the creeping region during the earthquake cycle. We derived for this analytical expressions to compute the viscoelastic response due to time-dependent creep. Although this model remains kinematic, it provides physical insights of the transitional region between the locked region and the top of the viscoelastic medium.

Using this improved model, we found solutions for fitting the surface deformation rates in the Carrizo Plain section of the San Andreas fault, that allow for reasonable estimates for earthquake

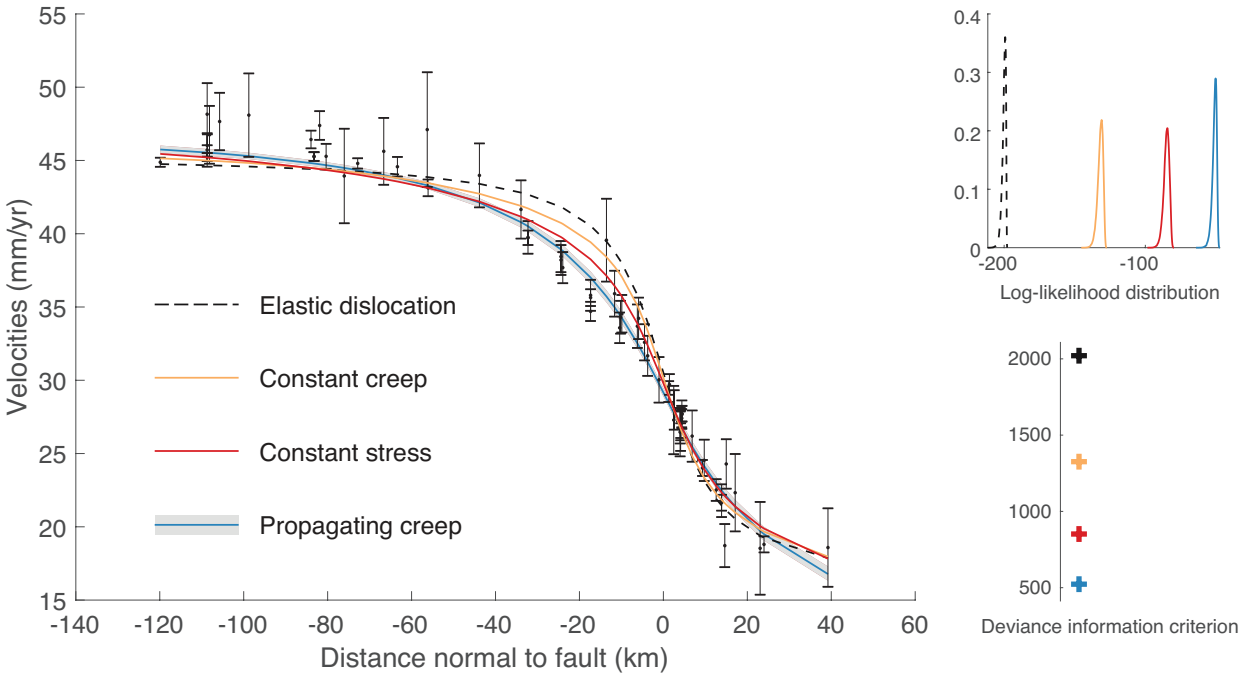

Figure 4: Best fitting models, log-likelihood distributions and corresponding deviance information criteria. Although the difference is small, our propagating creep model fits better the data set compared to other models.

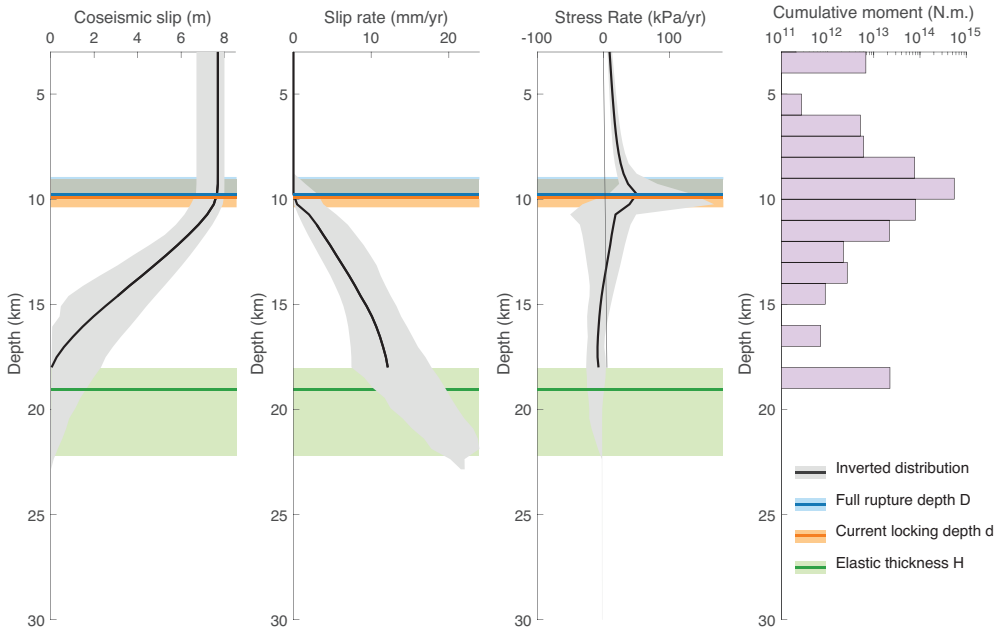

Figure 5: Distribution of coseismic slip, slip rate, stress rate, D, d and H for our improved model. Median solutions are indicated in bold lines, the 2-σ uncertainties are given by the shaded regions. We compare the obtained stress rate distribution to the cumulative moment from microseismicity between 1981 and 2016 along the Carrizo Plain (*Lin et al.*, 2007; *Hauksson et al.*, 2012).

rupture depth and coseismic displacement, with respect to the current microseismicity. Although this model was designed to account for a possible migration of the locking depth, best fitting solutions have very low propagation speeds, less than a meter per year, pointing to a lack of creep propagation. Future work should consider the use of additional data sets, such as microseismicity, repeating earthquakes, and tremor locations, to confirm and better constrain this behavior in fault systems. As a corollary, the difference in fit with models developed by *Johnson and Segall* (2004) where creep occurs at constant stress, does not seem to be caused by the additional creep propagation. The systemic better fit that is observed here might originate from the fact the model we developed, independently from the propagation, seems to provide a more flexible solution for creep rate distribution in the transitional region. This model could be used in the future as a guide for studying the state and temporal evolution of transitional region on strike-slip fault systems.

Supported bibliography

1. Bruhat, L. & P. Segall, Can deformation rates across the Carrizo Plain segment of the San Andreas Fault be explained by vertical migration of the locked-to-creeping transition? Abstract SCG53-14 presented at JpGU Meeting 2018, Chiba, Japan
2. Bruhat, L., & Segall, P. (2017, 08). Can deformation rates across the Carrizo Plain segment of the San Andreas Fault be explained by vertical migration of the locked to-creeping transition? . Poster Presentation at 2017 SCEC Annual Meeting. SCEC Contribution 7456
3. Bruhat, L. (2019). A physics-based approach of deep interseismic creep for viscoelastic strike-slip earthquake cycle models, submitted, https://doi.org/10.31223/osf.io/c4jnh.

References

Bruhat, L., and P. Segall (2017), Deformation rates in northern Cascadia consistent with slow up dip propagation of deep interseismic creep, *Geophysical Journal International*, doi:10.1093/gji/ggx317.

Hauksson, E., W. Yang, and P. M. Shearer (2012), Waveform Relocated Earthquake Catalog for Southern California (1981 to June 2011), *Bulletin of the Seismological Society of America*, *102*(5), 2239–2244, doi:10.1785/0120120010.

Johnson, K. M., and P. Segall (2004), Viscoelastic earthquake cycle models with deep stress-driven creep along the San Andreas fault system, *Journal of Geophysical Research: Solid Earth*, *109*(B10), doi: 10.1029/2004JB003096.

Lin, G., P. M. Shearer, and E. Hauksson (2007), Applying a three-dimensional velocity model, waveform cross correlation, and cluster analysis to locate southern California seismicity from 1981 to 2005, *Journal of Geophysical Research*, *112*(B12), B12,309, doi:10.1029/2007JB004986.

Savage, J. C., and W. H. Prescott (1978), Asthenosphere readjustment and the earthquake cycle, *Journal of Geophysical Research: Solid Earth*, *83*(B7), 3369–3376, doi:10.1029/JB083iB07p03369.

Segall, P. (2010), *Earthquake and volcano deformation*, Princeton University Press, Princeton, New Jersey.

Shen, Z.-K., R. W. King, D. C. Agnew, M. Wang, T. A. Herring, D. Dong, and P. Fang (2011), A unified analysis of crustal motion in Southern California, 1970-2004: The SCEC crustal motion map, *Journal of Geophysical Research: Solid Earth*, *116*(B11), n/a–n/a, doi:10.1029/2011JB008549.

Spiegelhalter, D. J., N. G. Best, B. P. Carlin, and A. van der Linde (2002), Bayesian measures of model complexity and fit, *Journal of the Royal Statistical Society: Series B (Statistical Methodology)*, *64*(4), 583–639, doi:10.1111/1467-9868.00353.